Available online at www.sciencedirect.com

ScienceDirect

Procedia Structural Integrity 62 (2024) 331–338

Structural Integrity Procedia

www.elsevier.com/locate/procedia

II Fabre Conference – Existing bridges, viaducts and tunnels: research, innovation and applications (FABRE24)

Parametric analysis of corrosion effects on strength of RC decks with post-tensioned tendons

Fabio Minghini[a]*, Marco Accolli[a], Andrea Fabbri[a], Marco Nale[a], Alessandro Ranzati[a]

[a]*University of Ferrara, Engineering Department DE, Via G. Saragat 1, Ferrara 44122, Italy*

Abstract

This investigation originates from extensive observational surveys conducted on RC highway viaducts located in Liguria Region, Italy. Some of these viaducts were recently subjected to significant retrofitting interventions including deck seismic isolation and piers restoration. However, at the time of surveys noticeable defects and degradation mechanisms were observed in some decks, with particular reference to simply supported RC I-beams with post-tensioned tendons. The main defects were the consequence of incorrect rainwater runoff due to obsolescence of drainage systems. Damages and corrosion in ducts for post-tensioned reinforcement were also observed in some case. Finally, in one case the surveys put in evidence broken wires belonging to a post-tensioned tendon of one of the outer beams. Given the well known critical issues related with existing post-tensioned reinforcement, a parametric analysis of the I-beams is carried out by varying the ratio of ineffective to total area of prestressing steel and, correspondingly, the amount of residual prestress. Nonlinear sectional analysis up to Ultimate Limit State in bending is implemented in program Response2000 (E. Bentz, University of Toronto). The effects due to pitting corrosion are accounted for by reductions in reinforcement area and suitable changes in steel constitutive model. Preliminary results show a satisfactory beam capacity provided that the prestressing steel is totally effective. Decreases in prestressing force and beam bending capacity are computed at different levels of corrosion attack, obtaining a comparative evaluation of crack patterns.

Keywords: Post-tensioning; Corrosion; Pitting; Bending capacity; Bridge deck

* Corresponding author. Tel.: +39-0532-974912; fax: +39-0532-974870.
E-mail address: fabio.minghini@unife.it

10.1016/j.prostr.2024.09.049

1. Introduction

Bridges play an important role in maintaining infrastructure functionality under both ordinary and emergency conditions (Nale et al., 2020). The publication of the Italian guidelines for existing bridges (Ministry of Infrastructures and Transports, 2020) has drawn attention to the assessment of the safety of bridges, particularly in light of recent failures of these structures, e.g. Polcevera viaduct (Calvi et al., 2021), Fossano viaduct and Caprigliola bridge (Scattarreggia et al., 2022). A large part of bridges inventory in Italy is characterized by structures built more than 50 years ago. This poses challenges for the structural engineer and the scientific community to evaluate the performance of these structures given the design code, the evolution of design, and the durability of these structures.

In particular, one of the prominent concerns is the degradation of the materials in these structures and their impact. Indeed, one of the main issues of reinforced concrete bridges is corrosion which significantly affects the durability and safety of the structures. Visible effects include the reduction of the cross-section area of steel bars, leading to indirect effects such as micro-cracking in the surrounding area to the steel bar by altering the interface between steel and reinforced concrete with possible spalling of the concrete. Additionally, one of the effects on concrete can be induced by carbonation, which reduces the compressive strength of concrete.

This contribution is aimed at a parametric analysis of the role of residual effective area of prestressing steel as well as of residual prestress on ultimate and serviceability limit states. In particular, the variation of bending moment capacity at the Ultimate Limit State (ULS) is analyzed, whereas the cracking moment and relative crack pattern are evaluated at the Serviceability Limit State (SLS).

This parametric analysis is systematically applied to case studies of highway bridges recently surveyed, located in Liguria, Italy. In particular, the study focused on the reinforced concrete beams under traffic loads. Notably, seismic loads are not considered in this preliminary analysis. As a matter of fact, similar structures have been retrofitted introducing seismic isolation bearings at the top of the piers.

2. The case studies of RC highway viaducts with post-tensioned tendons

The RC viaducts selected as case studies (Fig. 1) share the same structural typology showing I-section girders with post-tensioned tendons. These viaducts are also characterized by a similar grade of structural defects related with corrosion of reinforcement, which deserves an in-depth analysis. Pending specific tests suited to infer statistical distributions of corrosion attacks and residual area of reinforcement, a preliminary, parametric numerical investigation is carried out and presented in this paper.

Original design documents were available for both viaducts. The oldest of the two, comprised of two parallel, closely spaced viaducts. These structures, located in the province of La Spezia, were built in 1969. Therefore, the project adheres to the design requirements of the code of the time, i.e. Circular of the Ministry of Public Works n. 384 of 14/02/1962. The overall length is of 222 m, and is comprised of 6 spans, with an average span length of about 37 m. The generic span for each of the two decks consists of a group of three simply supported beams, connected with one another by five crossbeams and a 20 cm-thick top slab. The track width is 8.50 m, resulting in a total width of 9.63 m.

The decks are supported by single-cell circular box-section pier. Each of them rests on a shallow foundation comprised of 4 piles and a top footing. Finally, the abutments have a regular shape equal for both sides of the viaducts.

(a) (b) (c) (d)

Fig. 1. Selected case studies.

2.1. Geometry and material of bridge girders

The main beams of viaducts have average span length of 36.30 m, total height of 220 cm and, within the I-shaped portion, flange breadth of 70 cm and web thickness of 20 cm. In each of the beams, six tendons are present (Fig. 2). Five of them are composed of 44 ∅6. The remaining top tendon is comprised of 30 ∅6. A schematic of the longitudinal reinforcement is reported in Fig. 2a, whereas the shear reinforcement, comprised of 10 mm- and 12 mm-diameter vertical bars, is shown in Fig. 2b.

The I-shaped cross-section of the beams becomes rectangular near the supports, where a reduction in height is present to allow the positioning of neoprene rubber bearings. These bearings are placed on suited seats of height variable between 18 and 33 cm.

A typical cross-section of the bridge decks is illustrated in Fig. 3, whereas Table 1 reports material properties inferred partly by original design drawings and calculation reports and partly by recent tests on materials. In particular, these tests were carried out in view of the intervention for replacement of bearing devices.

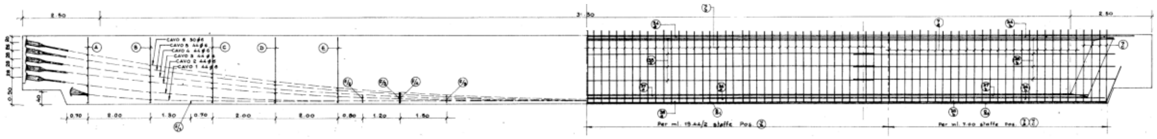

(a)

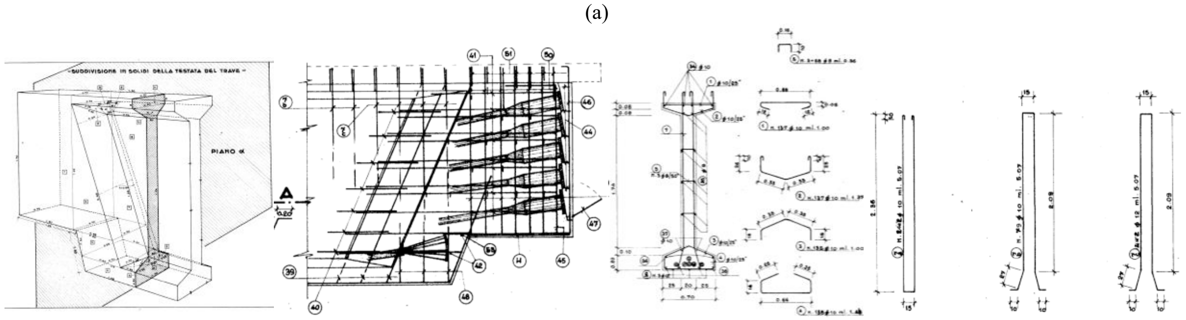

(b)

Fig. 2. RC beams (from original drawings): reinforcement details, (a) longitudinal section; (b) tendons anchorage and cross-section.

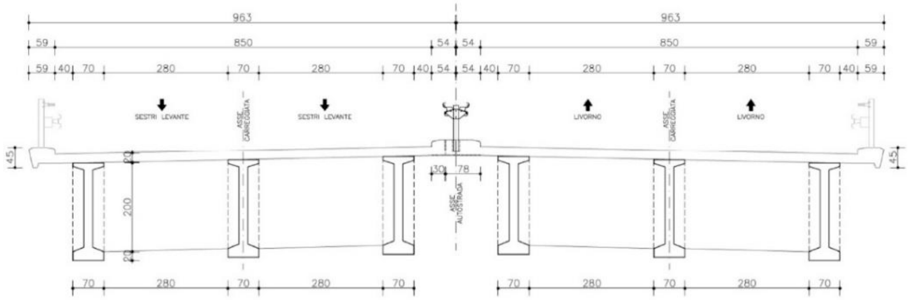

Fig. 3. Deck cross-section with prestressed concrete girders (from original drawings).

Table 1. Mechanical parameters of the materials.

Property	Symbol	Value
Characteristic cylinder compressive strength	f_{ck}	28 MPa
Design compression strength	f_{cd}	15.87 MPa
Modulus of elasticity of concrete	E_{cm}	32.31 MPa
Characteristic yield strength of rebar	f_{yk}	404.50 MPa
Design tensile strength of rebar	f_{yd}	351.74 MPa
Characteristic tensile strength of steel tendons	f_{pk}	1650 MPa

2.2. Defect detection

The viaducts present typical defects characterized by detachment of concrete portions, as well as by exposure and corrosion of the reinforcement. Whilst original bearings were recently replaced with seismic isolation bearings (Fig. 4a), some heavy defect still has remained at the time of survey, although further refurbishment interventions were in progress. Some of the observed defects (Fig. 4b-d) must be ascribed to insufficient concrete cover and inadequate drainage of rainwater. The most significant defects were those concerning the post-tensioning system (Fig. 5). Among them, exposure and degradation of ducts have been identified (Fig. 5a, b), and, in one case, the rupture of one tendon wire (Fig. 5c). These observations led to develop the parametric analysis illustrated in the next section.

(a) (b) (c) (d)

Fig. 4. Visual survey photo report of main elements of viaducts.

(a) (b) (c)

Fig. 5. Main defects observed in ducts and tendons.

3. Parametric Analysis

Parametric analysis focuses on a RC beam element with post-tensioned tendons and related effects of corrosion-induced cross-section area reduction for tendons. Unfortunately, the assessment of tendons residual cross-section area is an extremely complex task when relying upon visual inspections only. Indeed, only through tomographic investigations, endoscopes, and measurements of electrochemical potential, it is possible to determine the presence of voids in the ducts and the depth and speed of the corrosion itself. Here, a simplified numerical procedure is employed to evaluate the loss of load-bearing capacity in the beam accounting for corrosion. The corrosion model proposed by Jeon et al. (2019) has been used. This model measures the progress of corrosion based on the reduction of resistant areas of wires, or of cables, through the definition of appropriate pitting depths. at which the type of corrosion is occurring. In general, the loss of prestressing steel area entails a reduction of residual strength that can be related to the loss of weight, but is not correlated to the residual ductility (Finozzi et al. 2018). In the present case study, the application of this model is performed assuming that the corrosion acts only on the five 44 $\phi 6$ tendons, and identically for each tendon, thus obtaining a unique corrosion progress for all of the tendons. The process (Fig. 6) is supposed to originate from the lowest point of the transverse section of the tendon. Starting from the full section, a progressively increased corroded tendon area is obtained increasing pitting depth D_p. In the absence of specific measurements, it was chosen to simulate a corrosive process that affects up to 30% of the initial resistant tendon area, through the definition of seven successive corrosion steps for the following D_p values: 5 mm, 7.5 mm, 10 mm, 12.5 mm, 15 mm, 17.5 mm, and 21 mm. An alternative evaluation method based on the reduction of the resistant area and the probability of corrosion has been proposed in the recent Fabre guidelines (Consorzio Fabre, 2022).

A critical issue in the described model is represented by the internal arrangement of wires in the tendon. In this research, the arrangement shown in Fig. 6 was only supposed. However, subsequent studies should also take account of statistical variability of pitting effects depending on wires arrangement. A further aspect to be addressed will be the calibration of corrosion progress model and its correlation with the corrosion of individual wires.

For each corrosion step, the corroded area may include both entirely and partly corroded wires. The corroded area affects the overall mechanical parameters of the tendon: in this work, it was decided to consider the wires inside the corroded area as totally ineffective; at the same time, the wires crossed by the pitting surface are considered as characterized by a reduced cross-section and a decreased tensile strength, according to the following expression:

$$f_{u,c} = \xi(a\eta + b) \tag{1}$$

with a = -1991.8 MPa, b = 1748 MPa, $\eta = A_{corr}/A_0$ [-], and ξ =0.8847 [-] which has been introduced as a corrective factor to the formula proposed by Jeon et al. (2019). The previous equation allows computing a reinforcement steel strength accounting for loss cross-section area due to partial corrosion. Therefore, if a given wire lies inside the fully corroded region, its ultimate tensile strength is zero, i.e. $f_{u,c}$ = 0 MPa. Conversely, if the wire lies completely outside the corroded region, it is assumed as intact, i.e. $f_{u,c} = f_{pk}$ = 1650 MPa. Finally, if the wire is crossed by the pitting surface, it is assumed as partially corroded, and Eq. (1) applies.

Table 2 shows the tensile strengths for the 15 wires involved in the corrosion process, corresponding to the fifth corrosion step (D_p = 15 mm, Fig. 6f). The ultimate tensile strength for the tendon is thus calculated as a weighted mean as follows:

$$f_{u,c,eq} = \frac{\sum_{i=1}^{44} A_{res,i} f_{u,c,i}}{\sum_{i=1}^{44} A_{res,i}} = 1580.11 \text{ MPa} \tag{2}$$

where $A_{res,i}$ is the cross-sectional area of the i-th wire, and $f_{u,c,i}$ is the relevant characteristic tensile strength. The reduction in tendon resistance and cross-sectional area obviously involves losses in prestressing force, which necessarily should be accounted for in bridge deck analysis.

Table 2. Ultimate strength for D_p = 15 mm.

Wire No.	$A_{0,i}$ [mm²]	$A_{corr.,i}$ [mm²]	$A_{res.,i}$ [mm²]	$\eta_i = A_{corr.,i}/A_{0,i}$	$f_{u,c,i}$ [MPa]
1	28.27	28.27	0.00	1.00	0.00
2	28.27	28.27	0.00	1.00	0.00
3	28.27	15.61	12.66	0.55	573.32
4	28.27	28.27	0.00	1.00	0.00
5	28.27	28.27	0.00	1.00	0.00
6	28.27	28.27	0.00	1.00	0.00
7	28.27	15.61	12.66	0.55	573.32
8	28.27	0.00	28.27	0.00	1650.00
9	28.27	6.11	22.17	0.22	1165.90
10	28.27	19.88	8.39	0.70	307.25
11	28.27	19.88	8.39	0.70	307.25
12	28.27	6.11	22.17	0.22	1165.90
13	28.27	0.00	28.27	0.00	1650.00
14	28.27	0.00	28.27	0.00	1650.00
15	28.27	0.00	28.27	0.00	1650.00

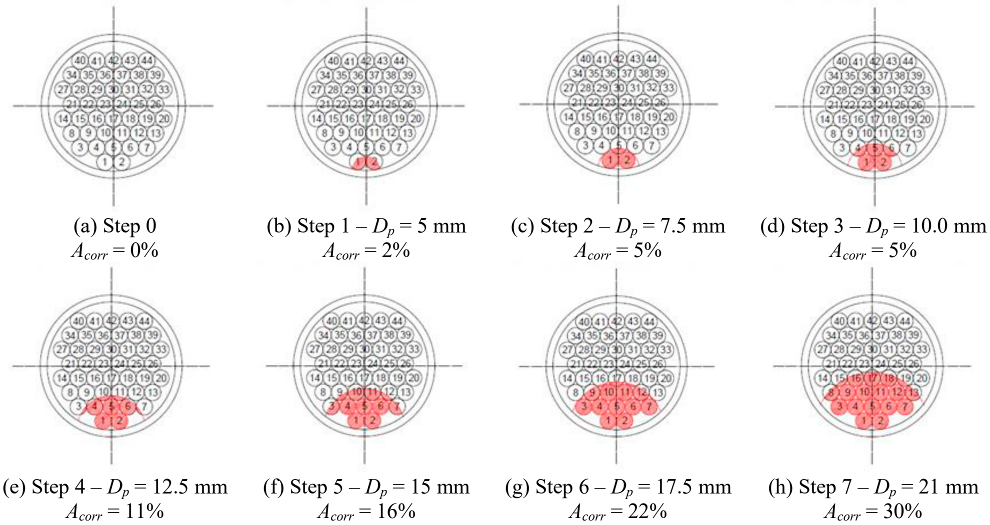

Fig. 6. Different levels of corrosion attack.

3.1. Assessment of cracking and ultimate bending moment resistances

In this section, the assessment of cracking and ultimate flexural strengths is evaluated as a function of the tendons corrosion state. For each corrosion state, the updated tendons stresses are computed. This leads to changes in the internal stress state of the beam. The losses in physical and mechanical properties of tendons therefore determines a new section configuration. It is obviously possible to calculate the cracking and ultimate moments for each corrosion state.

In Fig. 7 the variations of cracking moment M_{cr} and bending resistance M_{rd} due to changes in effective cross-sectional area of tendons A_p are shown. Both quantities are referred to bending resistance for entirely effective tendons. Long-term prestressing losses due to creep, shrinkage and relaxation are taken suitably into account as recommended in EN 1992-1-1:2004. The parametric analysis shows that for a 30% reduction in the tendons area, the bending capacity of the beam is reduced by about 33%. For the same A_p, a decrease in the first cracking moment approximately equal to 24% is observed.

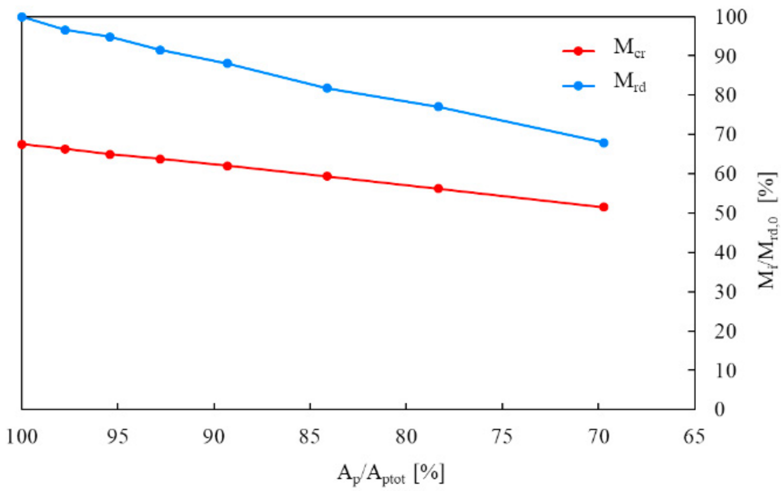

Fig. 7. Variations of cracking moment and moment resistance due to changes in effective tendons area.

Based on typical transversely-rigid deck models, the load configurations required by Italian standard D.M. 17/01/2018 were analyzed to locate the most unfavorable condition for the outer beams of viaducts. These preliminary analyses seem to indicate that a sufficient bending resistance is ensured in the case of entirely effective tendons only. Therefore, accurate inspection is absolutely needed to assess the actual corrosion tendons state. In addition, tests specifically suited to the estimate of residual prestressing force in tendons are necessary. In fact, the shear strength is strictly related to the mean compressive stress acting on the beam cross-section. The various resisting mechanisms involved in shear capacity of precast prestressed concrete members [Tullini and Minghini (2016), Tullini and Minghini (2020), Minghini and Tullini (2021)] are often affected by several uncertainties and then deserve particular attention. These features will be the subject of future developments.

3.2. Crack pattern analysis

A nonlinear analysis of a generic deck beam was then carried out up to the achievement of bending moment resistance to assess the crack pattern evolution. This analysis, conducted using the Response2000 software (Bentz, 2000), was performed for various corrosion states of tendons. The corresponding results are reported in Fig. 8.

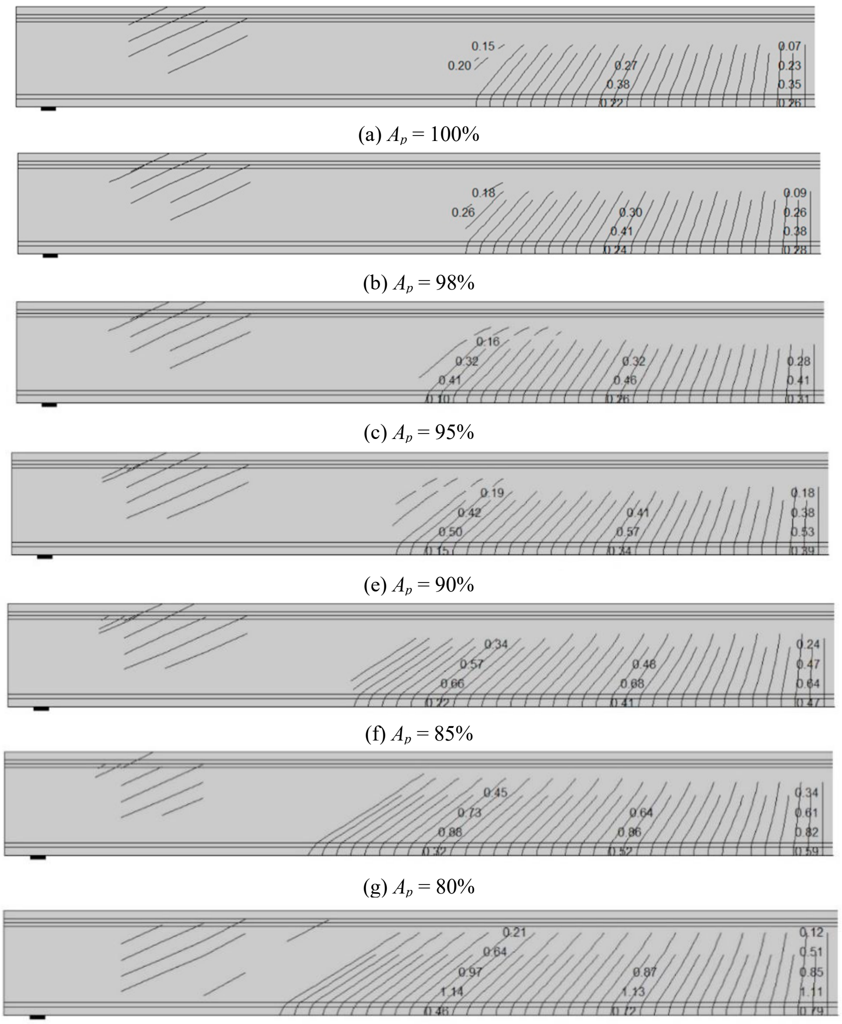

(a) A_p = 100%

(b) A_p = 98%

(c) A_p = 95%

(e) A_p = 90%

(f) A_p = 85%

(g) A_p = 80%

(h) A_p = 70%

Fig. 8. Beam crack patterns corresponding to different corrosion states.

Being tendons corrosion related to residual prestress, the crack patterns clearly show the increase in damage extension with loss of prestressing force.

4. Conclusions

This contribution presents a parametric analysis of the variation of the total area of prestressing steel for an I-beam, using previously surveyed RC viaducts as case studies. Loss area and property deterioration for prestressing steel globally correspond to reductions in the amount of residual prestress, which unavoidably affect both bending and shear beam capacities. Preliminary results indicate a satisfactory bending capacity, provided that tendons are entirely effective and subjected to the estimated long-term prestress.

This study forms the basis for further survey campaigns involving special inspection of prestressing force system, which should allow estimating the percentage of ineffective or deteriorated tendons. Statistical considerations on residual prestress, possibly accounting for the various sources of uncertainties, will then be used to calibrate a predictive numerical model of the bridge deck.

Acknowledgements

The authors gratefully acknowledge the financial support of the FABRE Consortium.

References

Bentz E. 2000. Sectional Analysis of Reinforced Concrete Members. Ph.D Thesis. Departement of Civil Engineering. University of Toronto, Canada.

Calvi G. M., Moratti M., Scattarreggia N., Özsaraç V., Calvi P. M., Pinho R. 2021. Numerical Investigations on the Collapse of the Morandi Bridge. In Developments in International Bridge Engineering: Selected Papers from Istanbul Bridge Conference 2018 (pp. 3-18). Springer International Publishing.

Consorzio Fabre, 2022. Ispezioni speciali su ponti esistenti in c.a.p. a cavi scorrevoli ai sensi delle Linee Guida: la classificazione e la valutazione accurata (in Italian)

Finozzi I., Saetta A., Budelmann, H. 2018. Structural response of reinforcing bars affected by pitting corrosion: experimental evaluation. Construction and Building Materials, 192, 478-488.

Jeon C. H., Lee J. B., Lon S., Shim C. S. (2019). Equivalent material model of corroded prestressing steel strand. Journal of Materials Research and Technology, 8(2), 2450-2460.

Minghini F., Tullini N. 2021. Seismic retrofitting solutions for precast RC industrial buildings struck by the 2012 earthquakes in Northern Italy. Frontiers in Built Environment, 7, 631315.

Ministry of Infrastructures and Transports. 2020. Ministerial Decree 578 on 17.12.2020. Adoption of Guidelines for the Classification and Management of Risk, the Safety Assessment and the Monitoring of Existing Bridges, Italy (in Italian)

Nale M., Chiozzi A., Tralli A., 2020. Stochastic Seismic Assessment of Bridge Networks by Matrix Based System Reliability Method. In Proceedings of XXIV AIMETA Conference 2019 24, 1559-1566. Springer International Publishing.

Scattarreggia N., Salomone R., Moratti M., Malomo D., Pinho R., Calvi G. M. (2022). Collapse analysis of the multi-span reinforced concrete arch bridge of Caprigliola, Italy. Engineering Structures, 251, 113375.

Tullini N., Minghini F. (2016). Grouted sleeve connections used in precast reinforced concrete construction–Experimental investigation of a column-to-column joint. Engineering Structures, 127, 784-803.

Tullini N., Minghini F. (2020). Cyclic test on a precast reinforced concrete column-to-foundation grouted duct connection. Bulletin of Earthquake Engineering, 18(4), 1657-1691.